IN-SITU PERFORMANCE EVALUATION BY SIMULATION OF A COUPLED AIR SOURCE HEAT PUMP/PV-T COLLECTOR SYSTEM.

Hachem Ben Nejma[1], Alain Guiavarch[1], Ismaël Lokhat[2], Eric Auzenet[3], Fabrice Claudon[4] and Bruno Peuportier[1]

[1]MINES ParisTech, CEP, Centre Energétique et Procédés, 60 Bd St Michel, 75272 Paris Cedex 06, France
[2]Cythelia, La Maison Zen, 350 route de la Traverse, 73 000 Montagnole, France
[3]CIAT Research & Innovation Centre BP14 – 01350 Culoz - France
[4]INES, 50 av. du Lac Léman, Savoie Technolac, 73375 Le Bourget du Lac, France

ABSTRACT

Thermal coupling between a heat pump and a hybrid photovoltaic thermal (PV-T) collector is efficient for two reasons. First the heat produced by the PV-T collector raises the temperature of the cold source of the heat pump, increasing its coefficient of performance. Secondly the PV collector can be cooled in a more efficient manner than in usual cases, which increases its efficiency.
The aim of the paper is to describe the work that has been done to evaluate by simulation the performance of such a system installed in a demonstration building.
Models have been developed for all components and coupled to a dynamic thermal simulation tool. Calculation has been compared to monitoring results, and then used to evaluate the performance of the installed system by comparison with the same building without the system.

INTRODUCTION

A photovoltaic collector produces thermal energy which can be recovered by air or water to heat the building (Tripanagnostopoulos, 2007) (Guiavarch, 2006). This solar component is generally described and modeled as a combination of a photovoltaic collector and an air solar collector, leading to what is commonly called a hybrid photovoltaic-thermal (PV-T) collector.

On the other hand, the coefficient of performance of an air source heat pump depends strongly on the ambient temperature, leading to a peak load on the electric public grid during winter. Filliard et al. (2009) showed by simulation that in some configurations it is possible to significantly improve the seasonal Coefficient of Performance (COP) of an air source heat pump, by coupling the external unit of the heat pump with temperate air-sources integrated into or near the building. This can be for instance an attic, a crawlspace, a sunspace, a heat recovery ventilation system, or an hearth-to-air heat exchanger.
The main idea developed in this paper is to transfer heat between the photovoltaic collector and the evaporator of the heat pump. Zondag (2001) studied how to preheat the air coming on the external unit of an air-to-air heat pump, and tested this concept into an experimental building. Candanedo and Athienetis (2008) simulated the performance of a water-to-water heat pump coupled with a building integrated photovoltaic system. In both aforementioned cases, the heat transfer between the photovoltaic collector and the external unit of the heat pump is made by convection. Some authors, as Ji et al. (2009) for instance, studied “direct” photovoltaic assisted heat pumps. In this case, the photovoltaic collector is directly coupled to the thermodynamic loop of the heat pump and acts as a radiative evaporator. The evaporation process cools the mc-Si cells, lowering their temperature, and raising their electrical efficiency.
All the aforementioned developments lead to the conclusion that the performance of this kind of system can be improved, but some limits remain. For instance, the solar production is not necessarily well correlated to the building heating load. The consequence is that a thermal storage device is necessary. The objective is to maximize the effective recovered thermal energy produced by the PV-T collector.

CASE STUDY DESCRIPTION

Building

The developed prototype has been installed in a new building called La Petite Maison Z.E.N (PMZ), which is a Zero Energy Net building (Figure 1). The 116 m² floor area are used for offices, and the building is located near Chambéry, in the French Alps.
It was designed to have a yearly overall primary energy consumption lower than 50 kWh/m².

Figure 1. Petite Maison Zen (Montagnole, Savoie, Cythelia consulting).

System

The system is illustrated in Figure 2. The three main parts are: the PV-T collector, the heat transfer from the PV-T collector to the heat pump, and the heat pump coupled to the storage tank.

The south oriented roof (70m²) is fully covered with a 7.2 kWp photovoltaic collector, made of 12% efficiency thin film CIGS modules. A 6 cm air gap allows for cooling the modules with a ventilation system described hereunder.

A air-to-water heat exchanger has been especially designed for this project, but using commonly manufactured products: one filter, one coil with six rows connected to the heat pump, and two variable speed plug fans mounted in parallel driven by electronically commutated motors. The requested available static pressure is 250 Pa for a maximum air flow rate of 3000 m^3/h (for the highest solar irradiance in summer). For those operating conditions, the input power, measured on a test bench before installation, is around 400 W. For the nominal air flow rate which is 1500 m^3/h, the input power is around 100 W.

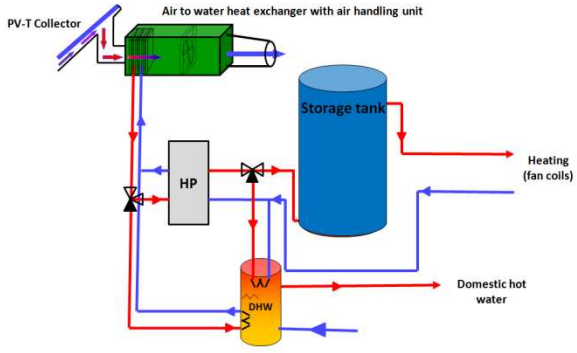

Figure 2. System description.

The selected heat pump is reversible and of water-to-water type (see Figure 3). The nominal heat capacity is 7.39 kW and the nominal COP is 5.10. The heat pump is connected to a 1000 litres storage tank, and in parallel, to a 300 litres tank for domestic hot water. The air-to-water heat exchanger can also be connected directly to the domestic water tank if the temperature is high enough. As the heat pump is reversible, the system is also able to cool the building in summer, but for simplification, in this paper, we concentrate only on heating.

Figure 3. Heat pump and storage tank.

SYSTEM COMPONENTS MODELLING

As introduced previously, the system consists mainly of a PV-T collector, a heat pump, and a water storage tank. The different corresponding models are developed and then coupled and implemented in a building simulation tool.

Photovoltaic-Thermal collector

The production of electricity by photovoltaic modules is calculated with the 1-diode model (Ricaud, 1997), assuming the collector is grid-connected. The characteristic curve I=f(V) is given by the following equation:

$$I = I_L - I_0 \left[exp\left(\frac{q}{\gamma k T_j} (V + IR_S) \right) - 1 \right] - \frac{V + IR_S}{R_{SH}}$$

where V and I are respectively the voltage and the current of the photovoltaic module, I_L is the photocurrent generated by the photovoltaic cells (A), I_0 is the diode saturation current (A), R_{sh} and R_s are respectively the shunt and series resistance (Ω), γ is an adjustment parameter (-).

We can also note that this equation depends on the junction temperature, which is equivalent to the operating temperature of the photovoltaic cells (and assumed to be uniform over the whole PV collector). The electrical efficiency depends on this junction temperature, which itself depends on the type of integration of the PV collector, and is given by a PV-T model, developed by Guiavarch (2006).

The PV-T model is able to represent many different types of integration of the PV collector in the building envelope: integration without thermal interaction with the building envelope (PV collector installed on a flat roof for instance); integration without air gap (PV collector directly integrated into the wall, and placed against an insulation for instance); and integration with a ventilated air gap (Figure 4).

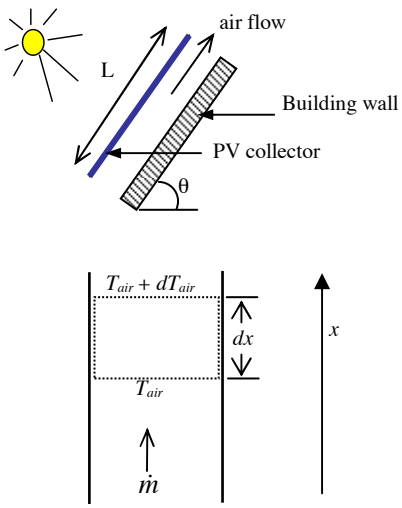

Figure 4. PV-T model illustration

In the case with a ventilated air gap, a model has been developed to calculate the thermal efficiency of the PV-T collector. This model assumes steady-state conditions (the thermal mass of the PV collector is neglected) and a one-dimensional conduction heat transfer perpendicular to the collector surface. The bulk air temperature varies according to the direction parallel to the air flow, and the mean outlet air temperature $T_{air,out}$ is calculated according to the mean inlet air temperature $T_{air,in}$. The heat transfer rate *q* is deduced, $\dot{m}$ being the mass air flow rate and *Cp* the specific heat of the air:

$$q = \dot{m} Cp \left(T_{air,out} - T_{air,in} \right)$$

In case of natural ventilation, several studies concerning the air flow in an air gap heated by a PV collector have been carried out. A rather simple method avoiding to use CFD (Computational Fluid Dynamics) type calculations allows to predict the air mass flow rate: a one-dimensional loop analysis in which the buoyancy forces are balanced by the pressure drops due to friction yields a third order polynomial equation. The calculation of the mass air flow rate $\dot{m}$ and q are inter-dependant and the solution is solved by using the Newton-Raphson method (Brinkworth et al., 2000).

Heat Pump

The heat pump model, whose heat balance is illustrated in Figure 5, is based on a steady-state empirical model and considers full load and part load conditions. A first set of equations is used to calculate the full load performance, for non rated conditions. The empirical model uses parameters which are deduced from manufacturer data.

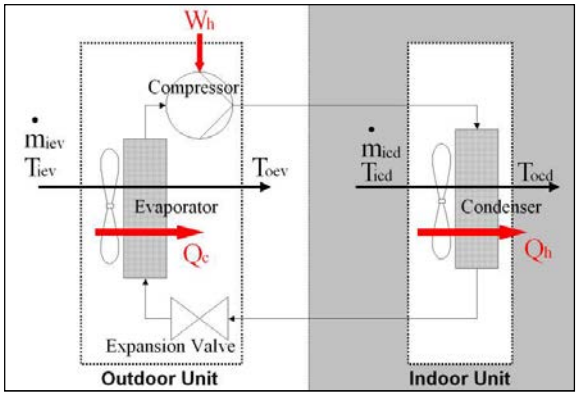

Figure 5. Heat pump energy balance

Assuming an isenthalpic process in the expansion device and no heat exchange between the system and its environment, in case of the heating mode we have:

$$\dot{Q}_{cd} = \dot{Q}_{ev} + \dot{W}$$

Where $\dot{Q}_{ev}$ is the evaporator heat transfer rate, $\dot{W}$ is the compressor power input and $\dot{Q}_{cd}$ is the condenser heat transfer rate.

A scroll compressor model is used. Several assumptions are incorporated into the modelling procedure:

- The compression and expansion in the compressor cycle are isentropic processes with equal and constant isentropic exponents
- The isentropic exponent is dependent on the refrigerant type
- The oil has negligible effects on refrigerant properties and compressor operation.
- There are isenthalpic pressure drops at the suction and discharge valves.

The theoretical power of the compressor $\dot{W}_t$ is given by :

$$\dot{W}_t = \frac{\gamma}{\gamma - 1} \cdot \dot{m}_r \, . P_{suc} \, . \nu_{suc} \cdot \left[\left(\frac{P_{dis}}{P_{suc}} \right)^{\frac{\gamma - 1}{\gamma}} - 1 \right]$$

Where $\dot{m}_r$ is the refrigerant mass flow rate (kg/s), γ is the isentropic exponent (-), P_{suc} is the suction pressure (Pa), ν_{suc} is the specific volume at suction state (m^3/kg), P_{dis} is the discharge pressure (Pa).

A simple linear representation has been used to account for the electrical and mechanical efficiency of the compressor. The actual power input for the compressor is calculated by the following equation:

$$\dot{W} = \eta \cdot \dot{W}_t + \dot{W}_{loss}$$

Where $\dot{W}$ is the compressor power input, $\dot{W}_{loss}$ is the constant part of the electromechanical power losses, η is the loss factor used to define the electromechanical loss that is supposed to be proportional to the theoretical power $\dot{W}_t$.
The condenser and evaporator models are developed from fundamental analysis of the counterflow heat exchangers. It is assumed that there is negligible pressure drop in the heat exchangers and, therefore, the refrigerant is at a constant temperature while changing phase. Since the temperature of the refrigerant in the two-phase region is considered constant, it is not necessary to differentiate whether the heat exchanger is actually counterflow or has some other configuration. The heat exchanger was treated as a simple heat exchanger with phase change on one side. The thermal effectiveness $\mathcal{E}$ is given by

$$\mathcal{E} = 1 - e^{-NTU}$$

Where $U = \frac{UA}{\dot{m} \cdot C_p}$. NTU is the number of transfer units, $\dot{m}$ is the mass flow rate of the fluid, and Cp is the specific heat of the fluid. UA is the heat transfer coefficient, which is assumed to be a constant independent of the fluid temperatures and flow rates.
The evaporating and condensing temperatures of the refrigerant are determined with the two following equations.

$$Q_{ev} = \varepsilon_{ev} . C_{p,w} \dot{m}_{w,ev} (T_{w,ev} - T_{ev})$$
$$Q_{cd} = \varepsilon_{cd} . C_{p,w} \dot{m}_{w,cd} (T_{w,cd} - T_{cd})$$

Where T_{ev} and T_{cd} are respectively the evaporating and condensing temperatures, $T_{w,ev}$ and $T_{w,cd}$ are respectively the evaporator entering water and the condenser entering water temperatures, $\dot{m}_{w,ev}$ and $\dot{m}_{w,cd}$ are respectively the water mass flow rate at the evaporator side and the condenser side, $C_{p,w}$ is the water heat capacity, and ε_{ev} and ε_{cd} are respectively the evaporator and the condenser thermal effectiveness.
The results calculated in full load conditions are then corrected to take into account the part load conditions, as illustrated in Figure 6. The part load factor (PLF) is the ratio between the real COP (coefficient of performance) and the COP calculated for full load conditions. This PLF is function of the part load ratio (PLR), defined as the ratio between the heating load of the building and the heating capacity of the heat pump at full load conditions. We see in Figure 6 that, for part load conditions (PLR < 1), the PLF is higher for inverter-driven heat pumps than for on-off heat pumps. Moreover, for inverter-driven heat pumps, the fan speed varies according to the part load ratio. Performance degradation due to frost formation is also accounted for. The reader can find more details in Filliard (2009).

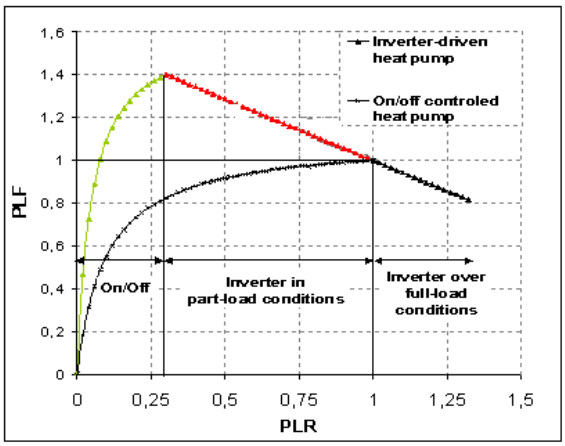

Figure 6. PLF versus PLR

Water tank

The model is derived from type 340 (Multiport store) from the TRNSYS library (Drück, 2006). In this model, it is assumed that the stratified hot water tank is divided into horizontal, thermally uniform water layers. Each one exchanges heat by conduction through the tank walls, and by conduction and convection between the adjacent water layers. The equations are detailed in Thiers (2008). Water can be injected in or extracted from any water layer. Assuming a perfect stratification, hot water injection is supposed to take place in the layer with the closest temperature. In the present model, cold water is injected in the bottom layer of the tank and hot water is extracted from the top layer.

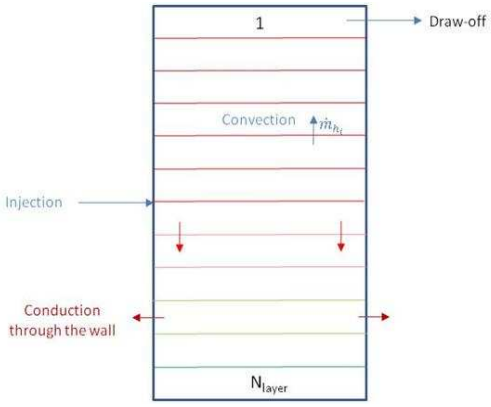

Figure 7. Stratified storage tank

The instantaneous power for a layer is given by the following equation

$$M_i \cdot C_{water} \cdot \frac{dT_i}{dt} = \sum_{j_i} \alpha_{j_i} \cdot \dot{m}_{j_i} C_{water} \cdot (T_{j_i} - T_i)$$
$$+\beta_{j_i} \cdot \dot{m}_{h_i} C_{water} \cdot (T_{i-1} - T_i)$$
$$+\gamma_{j_i} \cdot \dot{m}_{b_i} \cdot C_{water} \cdot (T_{i+1} - T_i)$$

$$+\frac{\lambda_{water}\cdot A_{layer}}{H_{layer}}\Big((1-\delta_i^1)\cdot(T_{i-1}-T_i) + \left(1-\delta_i^{N_{layer}}\right)\cdot(T_{i+1}-T_i)\Big) + UA_i\cdot(T_{amb}-T_i)$$

Where M_i is the water mass in a layer (kg) , $\dot{m}_{ji}$ is the injection or draw-off mass flow rate into the layer i by the port j (kg/s), $\alpha_{j_i}, \beta_{j_i}, \gamma_{j_i}$ are equal to 1 if the mass flow rate is positif and equal to 0 if the mass flow rate is null. T_{j_i} is the temperature of water injected into the layer i (K), λ_{water} is the water thermal conductivity (W/m/K), A_{layer} is the horizontal cross section of the store (m²),H_{layer} is the height of a layer (m), UA_i is the heat loss capacity rate (W/m), T_{amb} is the ambient temperature, δ_i^j is the Kronecker symbol.

Control

The control module is illustrated in Figure 8 (for the heating only). The heat pump and the air handling unit are switched on if the temperature of the storage tank is lower than a given threshold. The air handling unit can also be switched on (but without coupling with the heat pump) if the air temperature at the outlet of the PV-T collector is higher than a given threshold. It allows the PV-T collector to be cooled in summer. A more detailed view of the algorithm for the heating and domestic hot water can be found in (Ben Nejma, 2012).

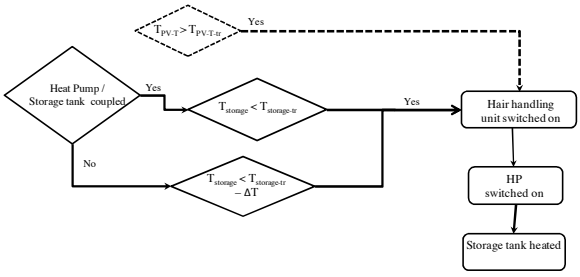

Figure 8. Simplified view of the control algorithm (for the heating only)

IMPLEMENTATION INTO A DYNAMIC THERMAL SIMULATION TOOL

The thermal simulation tool of multi-zone buildings named COMFIE allows heating and cooling loads as well as temperature profiles in different zones to be evaluated. It is based on a finite volume method, reduced after modal analysis (Peuportier and Blanc Sommereux, 1990). The program has been developed using an object oriented approach, allowing modules to be linked to the core of the program. These modules can represent building integrated photovoltaic systems, heat pumps or storage devices for instance (Figure 9).

During the simulation process, parameters are exchanged at each time step (typically between 1 hour and 10 minutes) between objects and/or the core of the program. A control module has been introduced to supervise the interaction between the different systems.

The cold air source temperature of the heat pump ($T_{cold\ source}$) is given by the outlet air temperature of the PV-T collector ($T_{air,PVT}$, depending on the ambient air temperature T_{air} and the incident solar irradiance G_{inc}). In summer, if $T_{air,PVT}$ exceeds a threshold value, the air handling unit is switched on to limit the junction temperature of the PV-T collector.

The control module determines if the heat pump is coupled to the heating loop of the building (*Coupling sate*). According to the coupling state, the storage tank temperature ($T_{storage}$), the building heating load (*Heating load*) and the heat produced by the PV-T collector, the heat pump module calculates the heating capacity (*HP heating capacity*) and its part load factor.

Figure 9 gives a simplified illustration of the coupling between the different components, but the interaction between them can be more complex. For instance, the heat balance of the PV-T collector is function of the temperature of the adjacent building zones.

In any case, an iterative algorithm is employed at each time step to ensure convergence, especially on the temperatures calculated by the different modules.

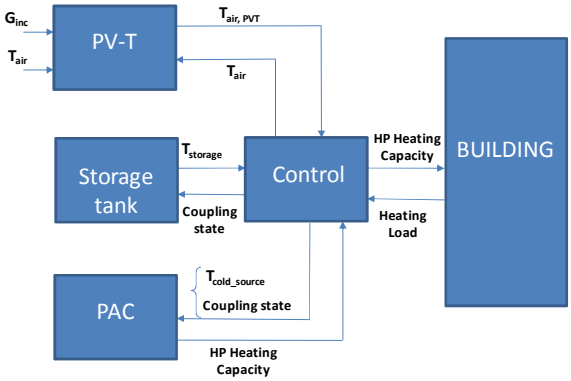

Figure 9 – Coupling of the different modules

The hourly outputs of the resulting simulation tool are for instance the absorbed energy and the COP of the heat pump. These results, once integrated over one year, will give the efficiency of the whole system. Other variables (hourly mean temperatures or electricity produced by the PV-T collector for instance) can also help to assess its performance.

USE OF THE SIMULATION TOOL IN THE DESIGN OF THE SYSTEM

The design of the system is the result of a collaborative work between researchers, engineers and technicians in the framework of a research project funded by the Agence Nationale de la Recherche. Figure 10 illustrates the use of the

simulation tool for the building model. The heating load is 22 kWh/m².

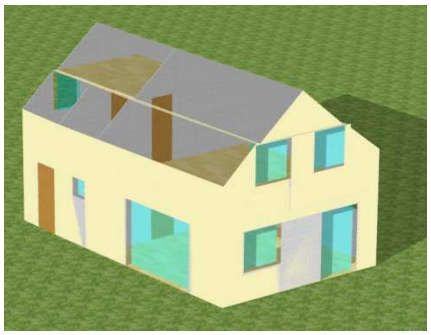

Figure 10. 3D view of the building model obtained with the simulation tool Pleiades-Comfie

The simulation tool described above has been used to help the research team for the design of the system. It was shown (Ben Nejma and Guiavarch, 2012) that the system is more efficient if the storage tank is placed at condenser side than if it is placed at the evaporator side.

Figures 11 gives the total (heat pump, air handling unit and other auxiliaries) yearly electrical consumption according to the air flow rate in the PV-T collector. It shows an optimum: for low air flow rates, the heat transfer is not efficient, and for higher air flow rates, the drop losses in the air circuit become too significant, raising the power consumed by the fans.

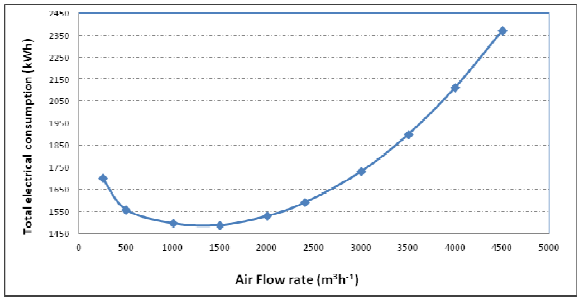

Figure 11. Total yearly electrical consumption according to the air flow rate in the PV-T collector.

Figure 12 shows the variation of the total yearly electrical consumption of the system according to the storage tank volume. It shows also an optimum (at around 1 m^3). If the volume is too small, the tank can't store enough energy and the electrical back-up of the system induces higher electrical consumption, but if the volume is too high, all the energy stored in the tank is not necessarily useful.

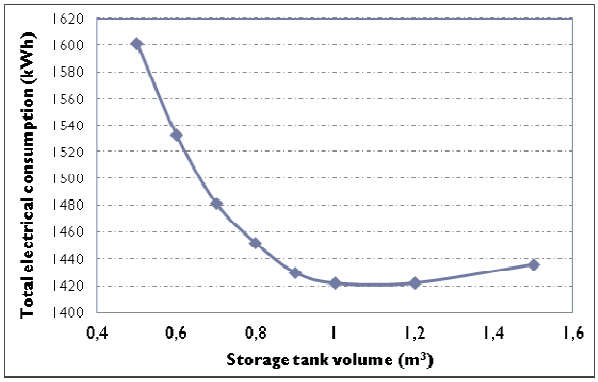

Figure 12. Total yearly electrical consumption according to the storage tank volume.

As already mentioned, this paper focuses on the heating load. Nevertheless, the system has also been designed for the domestic hot water and the cooling.

COMPARISON WITH MONITORING DATA

Figure 13 gives the comparison between the model and the monitoring results concerning the outlet air temperature of the PV-T collector, for 3 days of the first week of November 2011.

The figure shows a good agreement between the model and the experiment. The mean discrepancy between the model and the experiment is 0.7°C.

Nevertheless, we can note some discrepancy during the night, because the radiation heat exchange between the PV collector and the sky is not accurately taken into account in clear sky conditions.

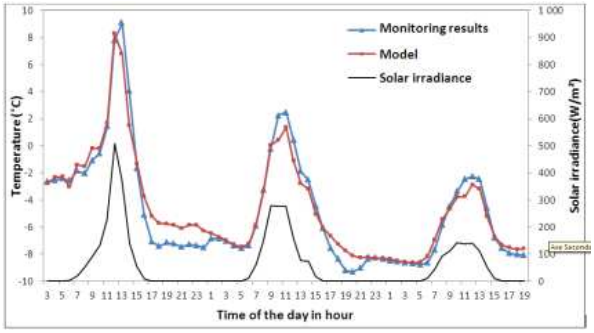

Figure 13. Outlet air temperature of the PV-T collector. Comparaison between the model and the monitoring results

Figure 14 gives the comparison between the model and the experiment for the coefficient of performance of the heat pump for one day of February 2012 (more (precisely from 12 pm to 4 pm). The figure shows a good agreement between the model and the experiment. The mean discrepancy between the model and the experiment is 1.3 %, the maximum discrepancy being 4 %.

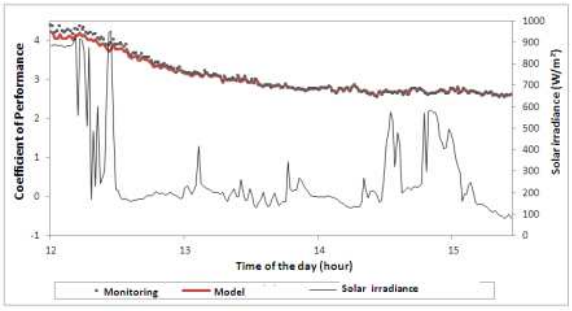

Figure 14. COP of the heat pump. Comparison between the model and the monitoring results

EVALUATION OF THE EFFICIENCY OF THE SYSTEM

It has been shown that the model of the system is in good agreement with the monitoring results measured in real operating conditions. It allows then to validate the complete model and to perform a yearly simulation of the whole installation, including the building heating load calculation. The results hereunder are given for heating only.

The system which has been described in this paper (PV-T/HP coupled) is simulated, as well as exactly the same system, but without thermal coupling between the PV-T collector and the heat pump (PV-T/HP not coupled). Both systems are compared to a reference system (PV/HP ref), composed of an on/off air to water heat pump and of an unventilated PV roof having the same size as the one installed on the demonstration building. In this reference system, no coupling exists between the heat pump and the PV-T collector and there is no water storage. The heating system as well as the building are kept identical in the three cases.

The PV-T/HP coupled system reduces the total yearly electrical consumption by around 20 % compared to the reference case. The gain of the PV-T/HP not coupled system compared to the reference case is only 7 %. It shows that the heat storage contributes for around 7% in the efficiency of the system, and the coupling between the PV-T collector and the heat pump contributes for around 13 %.

Table 1. Total yearly electrical consumption of the PV-T/HP coupled system, PV-T/HP not coupled system, and the reference PV/HP.

	Total yearly electrical consumption (kWh)	Gain (%)
Reference system	1459	-
PV-T/HP not coupled	1333	7
PV-T/HP coupled system	1182	20

CONCLUSION

The coupling between a PV-T collector and an air source heat pump has been studied. This paper showed how a dynamic thermal simulation tool has been used to help to design the system and its integration in a building. The discrepancy between monitoring data and results of the model of the global system integrated in the building was for instance less than 4% regarding the coefficient of performance of the heat pump. According to the calculations, the coupled PV-T/Heat pump system reduces the total electrical consumption by 20 % compared to the same building without this system. Further studies are planned to be done for assessing the efficiency of the system for the domestic hot water and for the cooling. This simulation tool can be used to study other case studies with different systems sizing, or to perform further optimisation studies.

ACKNOWLEDGEMENT

This work has been supported by the French Research National Agency (ANR) through the Habitat Intelligent et Solaire Photovoltaïque program (project PACAirPV n°ANR-08-HABISOL-005)

REFERENCES

Ben Nejma H., Guiavarch A., 2012. Etude de la performance d'un système couplant une PAC eau/eau avec un capteur hybride PV-T. AUGC-IBPSA Conference, 2012.

Brinkworth, B. J., Marshall, R. H., and Ibarahim, Z., 2000. A validated model of naturally ventilated PV cladding. Solar Energy. 69, 67-81.

Candanedo J. A, Athienitis A. K., 2008. Simulation of the performance of a BIPV-T system coupled to a heat pump in a residential heating application, 9th International IEA Heat Pump Conference, Zürich, Switzerland, 20-22 May 2008.

Drück H., 2006. MULTIPORT Store – Model for TRNSYS: Type 340, Version 1.99F, Universität Stuttgart, Institut für Thermodynamik und Wärmetechnik.

Filliard B., Guiavarch A., Peuportier B., 2009. Performance evaluation of an air-to-air heat pump coupled with temperature air sources integrated into a dwelling, Building Simulation Conference, Glasgow.

Guiavarch, A. and Peuportier, B., 2006 Photovoltaic collectors efficiency according to their integration in buildings, Solar Energy 80, 65–77.

Jie Ji, Hanfeng He, Tintai Chow, Gang Pei, Wei He, Keliang Liu., 2009. Distributed dynamic modelling and experimental study of PV evaporator in a PV-T solar-assisted heat pump.

International Journal of Heat and Mass Transfer, vol. 52.

Peuportier, B., and Blanc Sommereux, I., 1990. Simulation tool with its expert interface for the thermal design of multizone buildings, International Journal of Solar Energy, 8.

Ricaud A., 1997. Photopiles solaires; Presses Polytechniques et Universitaires Romandes, Lausanne.

Thiers S., 2008. Energy and environmental assessments of positive energy buildings, Ph.D. Thesis, Center for Energy and Processes, Mines ParisTech.

Tripanagnostopoulos, T., 2007. Aspects and improvements of hybrid photovoltaic/thermal solar energy systems, Solar Energy, 81-9.

Zondag H. A, 2001. Combined pv-air collector as heat pump preheater. 9th International Conference on Solar Energy in High Latitudes. Northsun 2001, Leiden, The Netherlands, 6-8 May, 2001.